Article

Cell

Broadly Neutralizing Alphavirus Antibodies Bind an Epitope on E2 and Inhibit Entry and Egress

Graphical Abstract

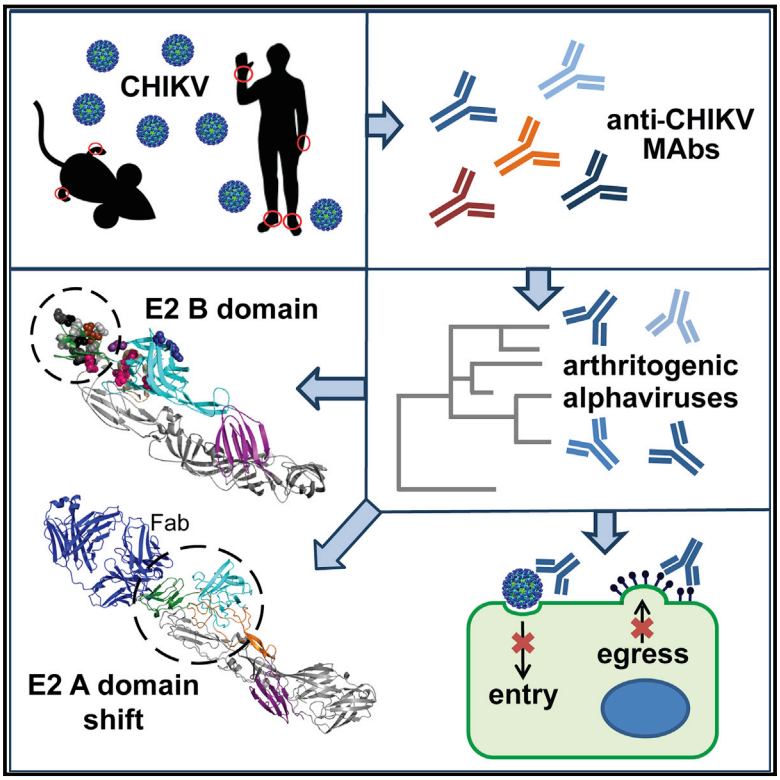

Highlights

- Broadly neutralizing MAbs bind an epitope in the B domain of alphavirus E2 protein
- Broadly neutralizing MAbs protect in vivo against infection by multiple alphaviruses
- B domain MAb binding re-positions the A domain and cross-links adjacent E2 spikes
- MAbs that cross-neutralize alphavirus infection block viral entry and egress steps

Authors

Julie M. Fox, Feng Long, Melissa A. Edeling, ..., Daved H. Fremont, Michael G. Rossmann, Michael S. Diamond

Correspondence

diamond@wusm.wustl.edu

In Brief

A class of broadly neutralizing monoclonal antibodies identified here protects against infection and disease in vivo against multiple alphaviruses, including chikungunya. These antibodies bind a discrete epitope on the alphavirus E2 glycoprotein, block viral entry and egress, and allow cross-linking of adjacent E2 protein spikes, suggesting avenues for possible vaccine- or antibody-based therapeutic development against multiple alphaviruses.

Accession Numbers

5ANY, EMD-3144

Fox et al., 2015, Cell *163*, 1095–1107
November 19, 2015 ©2015 Elsevier Inc.
http://dx.doi.org/10.1016/j.cell.2015.10.050

Cell

Broadly Neutralizing Alphavirus Antibodies Bind an Epitope on E2 and Inhibit Entry and Egress

Julie M. Fox,[1] Feng Long,[5] Melissa A. Edeling,[2] Hueylie Lin,[1] Mareike K.S. van Duijl-Richter,[6] Rachel H. Fong,[7] Kristen M. Kahle,[7] Jolanda M. Smit,[6] Jing Jin,[8] Graham Simmons,[8] Benjamin J. Doranz,[7] James E. Crowe, Jr.,[9] Daved H. Fremont,[2] Michael G. Rossmann,[5] and Michael S. Diamond[1,2,3,4,*]

[1]Department of Medicine
[2]Department of Pathology and Immunology
[3]Department of Molecular Microbiology
[4]Center for Human Immunology and Immunotherapy Programs
Washington University School of Medicine, St. Louis, MO 63110, USA
[5]Department of Biological Sciences, Purdue University, West Lafayette, IN 47907, USA
[6]University of Groningen and University Medical Center Groningen, 9713 GZ Groningen, the Netherlands
[7]Integral Molecular, Inc., Philadelphia, PA 19104, USA
[8]Blood Systems Research Institute, San Francisco, CA 94118, USA
[9]Departments of Pediatrics, Pathology, Microbiology, and Immunology and the Vanderbilt Vaccine Center, Vanderbilt University, Nashville, TN 37235, USA
*Correspondence: diamond@wusm.wustl.edu
http://dx.doi.org/10.1016/j.cell.2015.10.050

SUMMARY

We screened a panel of mouse and human monoclonal antibodies (MAbs) against chikungunya virus and identified several with inhibitory activity against multiple alphaviruses. Passive transfer of broadly neutralizing MAbs protected mice against infection by chikungunya, Mayaro, and O'nyong'nyong alphaviruses. Using alanine-scanning mutagenesis, loss-of-function recombinant proteins and viruses, and multiple functional assays, we determined that broadly neutralizing MAbs block multiple steps in the viral lifecycle, including entry and egress, and bind to a conserved epitope on the B domain of the E2 glycoprotein. A 16 Å resolution cryo-electron microscopy structure of a Fab fragment bound to CHIKV E2 B domain provided an explanation for its neutralizing activity. Binding to the B domain was associated with repositioning of the A domain of E2 that enabled cross-linking of neighboring spikes. Our results suggest that B domain antigenic determinants could be targeted for vaccine or antibody therapeutic development against multiple alphaviruses of global concern.

INTRODUCTION

Alphaviruses are arthropod-transmitted single-stranded positive-sense-enveloped viruses of the *Togaviridae* family and cause disease worldwide. The two surface glycoproteins on the mature virion, E2 and E1, facilitate binding and entry through receptor-mediated endocytosis and low-pH-mediated fusion within endosomes (Lescar et al., 2001; Smith et al., 1995). Alphavirus virions have T = 4 quasi-icosahedral symmetry, with 240 copies of the E2-E1 heterodimer assembling into 80 trimeric spikes on the viral surface (Cheng et al., 1995). Twenty of these spikes ("i3") are coincident with the icosahedral 3-fold axes, and 60 are in general positions at quasi 3-fold axes ("q3"). X-ray crystallographic structures have been determined of the E1 glycoprotein, the p62-E1 precursor, the E2-E1 heterodimer, and the $(E1\text{-}E2)_3$ trimer (Lescar et al., 2001; Li et al., 2010; Roussel et al., 2006; Voss et al., 2010). The mature E2 protein contains three domains: an A domain, which is located centrally on the surface of the spike and possesses the putative receptor binding site; the B domain, located on the distal end of the spike, covering the fusion loop on E1; and the C domain, at the proximal end of the spike. The E1 protein is a type II membrane fusion protein containing three β-barrel domains. Domain I is located spatially between domains II and III, with the fusion peptide lying at the distal end of domain II (Lescar et al., 2001; Voss et al., 2010). The E1 protein lies at the base of the trimeric spike with E2 positioned on top of it.

Chikungunya virus (CHIKV) is transmitted to humans by *Aedes* species of mosquitoes and causes a debilitating infection characterized by fever, rash, myositis, and arthritis, with joint disease lasting in some individuals for several years (Schilte et al., 2013). CHIKV historically caused outbreaks in Africa and Asia. In 2013, transmission of CHIKV occurred in the Western Hemisphere, and in just 18 months, CHIKV has caused more than 1.4 million cases in the Americas in more than 40 countries, including locally acquired infections in Florida (Kendrick et al., 2014). In comparison, other arthritogenic alphaviruses (e.g., Ross River [RRV], Semliki Forest [SFV], Mayaro [MAYV], and Sindbis [SINV] viruses) circulate with more limited global distribution, with outbreaks in Oceania, Africa, and South America.

Although currently there are no available licensed vaccines or therapies for CHIKV or any other alphavirus, studies have demonstrated the importance of antibody-mediated protection (Kam et al., 2012; Lum et al., 2013). Passive transfer of γ-globulin purified from the plasma of CHIKV-immune patients to mice

Table 1. Cross-Reactivity of Mouse and Human MAbs against Different Alphaviruses[a]

Antibody	CHIKV	ONNV	RRV	MAYV	SFV	UNAV	BEBV	GETV	MIDV	BFV
% E2 Identity		83.0	56.6	56.2	57.6	54.5	56.4	54.3	51.3	41.8
CHK-48	++	++		++		++	++	++		
CHK-65	++			++	++	++		++		
CHK-77	++	++		++	++	++	++	++		
CHK-88	++			++	++	++	++	++		
CHK-96	++	++					++	++		
CHK-98	++			++			++			
CHK-105	++					++		++		
CHK-124	++			++	++	++	++	++		
CHK-187	++	++	++	++	++	++	++	++		
CHK-265	++	++	++	++	++	++	++	++		
1I9	++	++	++	++				++	++	++
2C2	++	++	++	++				++		
2D12	++	++	++	++	++	++	++	++		
2H1	++	++		++						
4B8	++	++				++				
5F10	++	++		++		++				
8I4	++	++	++	++		++	++			
9D14	++	++	++	++	++	++	++	++	++	

CHIKV, Chikungunya virus; ONNV, O'nyong'nyong virus; RRV, Ross River virus; SFV, Semliki Forest virus; MAYV, Mayaro virus; UNAV, Una virus; GETV, Getah virus; BEBV, Bebaru virus; MIDV, Middelburg virus; and BFV, Barmah Forest virus. See also Figures S1 and S2.

[a]"++" denotes positive staining, and an absence of a symbol denotes negative staining by flow cytometry on infected cells.

prevented mortality following a lethal CHIKV infection (Couderc et al., 2009). Analogously, monoclonal antibodies (MAbs) neutralize CHIKV infection in vitro and protect against disease in mice and non-human primates (Fong et al., 2014; Fric et al., 2013; Goh et al., 2013; Pal et al., 2013, 2014; Smith et al., 2015).

One goal of vaccine and therapeutic efforts against viruses is the development of broadly neutralizing antibodies that inhibit most strains within a genetically diverse virus family. Broadly neutralizing MAbs have been described for human immunodeficiency (HIV), influenza A (IAV), dengue (DENV), and hepatitis C (HCV) viruses (reviewed in Corti and Lanzavecchia, 2013). Although broadly neutralizing MAbs against alphaviruses have not been described, polyclonal antibodies (induced by a CHIKV vaccine candidate) protected against O'nyong'nyong virus (ONNV) infection (Partidos et al., 2012) and convalescent serum from RRV-infected mice protected against CHIKV pathogenesis (Gardner et al., 2010). Earlier reports described cross-protection between different alphaviruses using hyperimmune serum (Wust et al., 1987). These studies suggest that conserved epitopes exist across different alphaviruses that are recognized by protective antibodies.

We screened a panel of murine and human MAbs against CHIKV (Pal et al., 2013; Smith et al., 2015) for neutralization of different alphaviruses. We identified ten MAbs that neutralized at least two different alphaviruses and showed that these MAbs blocked multiple steps in the viral lifecycle, including entry and egress. Two broadly neutralizing MAbs, CHK-187 and CHK-265, protected in vivo against CHIKV, ONNV, and MAYV. Genetic analyses established that broadly neutralizing anti-alphavirus MAbs recognized an epitope centered on the B domain of the E2 protein. Cryo-electron microscopic studies showed that binding of CHK-265 to the B domain on CHIKV was associated with repositioning of the A domain away from its native position in the E2-E1 heterodimer, which facilitated interaction with an edge of the A domain and cross-linking of adjacent E2 protein spikes. Overall, these studies describe a class of broadly neutralizing antibodies with protective activity that inhibit entry and egress of distantly related viruses within the alphavirus genus.

RESULTS

Anti-CHIKV MAbs Cross-Neutralize Related Arthritogenic Alphaviruses

Previously, we identified a panel of neutralizing mouse and human MAbs that inhibited infection of multiple CHIKV strains (Pal et al., 2013; Smith et al., 2015). As a first step toward evaluating whether MAbs against CHIKV had inhibitory activity against distinct alphaviruses with envelope protein amino acid identities ranging from 42.2% to 86.3% (Figure S1), we assessed immunoreactivity by flow cytometry (Figure S2). From the panel of 60 neutralizing anti-CHIKV MAbs, ten mouse MAbs and eight human MAbs bound to three or more different viruses (Table 1). However, these cross-reactive MAbs did not bind to cells infected with Venezuelan equine encephalitis virus (data not shown), which is more divergent (45.3% amino acid identity with CHIKV).

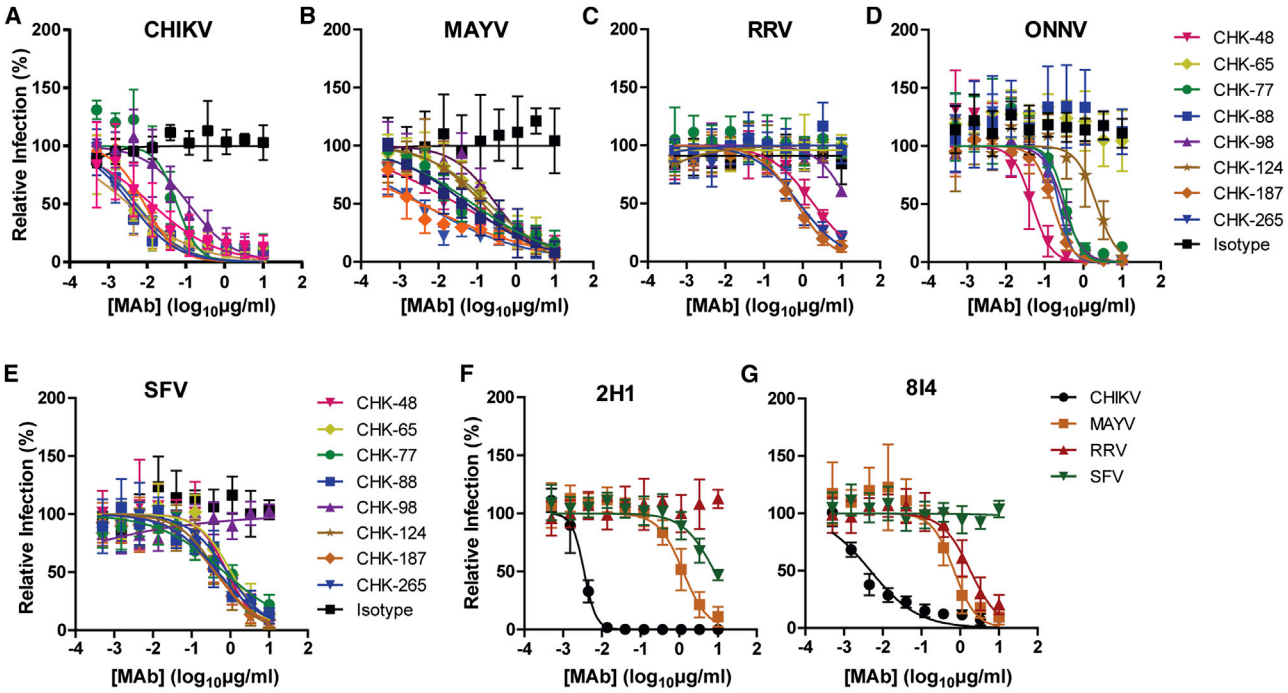

H

Antibody	CHIKV	MAYV	RRV	SFV	ONNV
CHK-48	13 (6-27)	32 (20-52)	1876 (1244-2827)	837 (536-1307)	48 (30-75)
CHK-65	5 (4-8)	202 (123-332)	>10,000	1055 (731-1523)	>10,000
CHK-77	59 (38-92)	78 (49-124)	>10,000	701 (435-1132)	342 (228-515)
CHK-88	4 (3-6)	55 (33-92)	>10,000	482 (303-768)	>10,000
CHK-98	118 (72-194)	308 (210-452)	>10,000	>10,000	298 (229-389)
CHK-124	3 (2-6)	140 (87-226)	>10,000	455 (315-658)	2210 (1475-3311)
CHK-187	9 (7-11)	4 (2-8)	694 (546-883)	403 (270-599)	160 (134-192)
CHK-265	5 (4-7)	4 (2-8)	812 (515-1280)	838 (564-1246)	234 (166-330)
2H1	4 (3-4)	1254 (934-1684)	>10,000	8147 (5676-11690)	N.D.
8I4	5 (4-7)	693 (439-1094)	1824 (1340-2484)	>10,000	N.D.

Figure 1. Murine and Human Anti-CHIKV MAbs Neutralize Infection of MAYV, RRV, ONNV, and SFV

(A–G) MAbs were incubated with 10^2 FFU of (A, F, G) CHIKV, (B, F, G) Mayaro, (C, F, G) Ross River, (D) O'nyong'nyong, or (E, F, G) Semliki Forest viruses for 1 hr at 37°C followed by addition of MAb-virus mixture to Vero cells for 18 hr. Virally infected foci were stained and counted. Wells containing MAb were compared to wells containing no MAb to determine the relative infection. DENV1-E98 was included as an isotype control MAb.

(H). EC_{50} values were determined by non-linear regression and are shown as ng/ml (95% CI). Each graph represents the mean and standard deviation (SD) from at least two independent experiments.

See also Figure S1.

We evaluated the neutralization potential of the cross-reactive MAbs against alphaviruses that are closely (ONNV) or distantly (MAYV, RRV, and SFV) related to CHIKV. As anticipated, each of the MAbs neutralized CHIKV infection efficiently (Figures 1A and 1H), as reported previously (Pal et al., 2013; Smith et al., 2015). Of the ten cross-reactive mouse MAbs tested, eight neutralized MAYV, seven neutralized SFV, six neutralized ONNV, and three neutralized RRV (Figures 1B-1E and 1H). Unexpectedly, cross-neutralization of MAYV was greater than ONNV even though the latter virus is more closely related to CHIKV (Figure S1). Three MAbs (CHK-48, CHK-187, and CHK-265) neutralized all alphaviruses tested, with CHK-187 and CHK-265 showing the greatest potency (Figure 1H). Of the eight cross-reactive human MAbs tested, only two (2H1 and 8I4) cross-neutralized MAYV, RRV, and/or SFV (Figure 1F and 1G). The sequences of human MAb 8I4 antibody variable genes were conventional; it used the most commonly expressed V_H gene (V_H3-23), had a high level of identity with germline sequences (99% [278 of 282 nucleotides] with V_H3-23*04 and 90% [45 of 50 nucleotides] with JH5*02), and had an HCDR3 length of 18.

Broadly Neutralizing MAbs Protect In Vivo against Multiple Alphaviruses

We assessed the efficacy of CHK-187 and CHK-265 in vivo against CHIKV using an arthritis model in wild-type (WT) mice (Morrison et al., 2011). A single 100 µg dose of CHK-187,

CHK-265, or an isotype control MAb was administered 1 day prior to infection with 10^3 FFU of CHIKV in the footpad. Treatment with CHK-187 or CHK-265 reduced ankle joint swelling to nearly baseline at 3 days after infection when compared to the isotype control MAb (Figure 2A). CHK-187 diminished the CHIKV burden in the ipsilateral ankle and prevented virus dissemination, whereas CHK-265 reduced spread to the contralateral ankle joint (Figure 2B).

Since the greatest cross-neutralization by CHK-265 or CHK-187 was against MAYV, we assessed the protective efficacy of these two MAbs in vivo against MAYV infection. To do this, we developed a new arthritis model of MAYV in WT mice. After inoculation with 10^3 FFU of MAYV, mice developed joint swelling, similar to that observed after CHIKV infection. Using this model, 100 μg of CHK-265, CHK-187, or an isotype control MAb was administered 1 day prior to infection, and ankle size was measured. Additionally, serum, spleen, quadriceps muscle, and ankles were collected on day 3 after infection. Treatment with CHK-265 or CHK-187 reduced joint swelling compared to isotype control MAb-treated animals (Figure 2C). The reduced disease correlated with decreased viral burden, as CHK-187 diminished viral load in the spleen, muscle, and contralateral ankle (Figure 2D). Remarkably, CHK-265 completely protected against MAYV infection, with no detectable virus at the site of inoculation or in any other tissue analyzed.

As an additional test, we evaluated the efficacy of CHK-265 and CHK-187 against ONNV infection. Since ONNV does not replicate extensively in WT mice (Seymour et al., 2013), we developed an arthritis model in *Ifnar*$^{-/-}$ immunodeficient mice. After infection with ONNV, *Ifnar*$^{-/-}$ mice developed ankle swelling and hind limb weakness, with variable rates of recovery. All mice receiving the isotype control MAb developed joint swelling and limb weakness. In contrast, mice receiving CHK-187 or CHK-265 showed minimal clinical disease (Figure 2E), reduced joint swelling from day 5 through day 14 after infection (Figure 2F), and greater weight gain (Figure 2G). To confirm that reduced disease was linked to decreased ONNV infection, we measured viral burden in the spleen, quadriceps muscles, and ankles 5 days after infection. CHK-187 reduced ONNV infection in the ipsilateral foot as well as at distant sites compared to isotype control MAb-treated animals (Figure 2H). CHK-265 limited ONNV spread to the contralateral joint and muscle. Thus, at least two broadly neutralizing MAbs can protect against infection and disease caused by multiple arthritogenic alphaviruses.

Cross-Protective MAbs Map to the B Domain of the E2 Glycoprotein

The binding sites of broadly neutralizing mouse and human MAbs were mapped by alanine-scanning mutagenesis and mammalian cell display (Davidson and Doranz, 2014) of the E2, 6K, and E1 proteins (Figure S3). All cross-neutralizing MAbs bound primarily to sites within the B domain of the E2 protein (Figures 3A and 3B). Eight amino acids (Q184, S185, I190, V197, Y199, G209, L210, I217) emerged as critical for binding (Figure 3A and 3B). These residues are highly conserved across CHIKV E2 proteins, as determined by alignment of 415 genome sequences (http://www.viprbrc.org) (Figure 3C). Variation was detected only at amino acid position 210 on E2, with leucine in 386 of 415 sequences, glutamine in 28 of 415 sequences, and threonine in 1 of 415 sequences. Alignment of other arthritogenic alphaviruses with CHIKV showed that I190, Y199, G209, and I217 are conserved, whereas Q184, S185, V197, and L210 are divergent, particularly in RRV (Figure 3A).

To corroborate the alanine-scanning mapping results, we introduced amino acid substitutions into CHIKV E2 ectodomain and generated recombinant proteins in *E. coli* (Pal et al., 2013) for binding studies (Figures 4A–4J). Amino acids in CHIKV E2 B domain were changed to the corresponding amino acids in RRV (Q184T, S185A, V192A, N193G) to previously defined escape mutations (G209E, L210P, K215E, K233E) against other neutralizing mouse MAbs or to residues (R68A and D250A) in the E2 A domain that showed loss of binding to other human MAbs (Pal et al., 2013; Smith et al., 2015). Binding of CHK-84, which maps to the A domain (data not shown), was not altered by any of the mutations, suggesting that the recombinant proteins folded correctly (Figure 4D). The majority of the E2 protein residues identified by alanine-scanning mutagenesis as part of the epitope (Figure 3A) were confirmed, and additional substitutions (e.g., Q184T, G209E, and L210P) that disrupted binding were detected. Binding of all cross-neutralizing MAbs tested was affected to varying levels by mutations at Q184, G209, and L210 (Figures 4A–4J). Mutation at S185 also was associated with loss of binding of several broadly neutralizing MAbs (Figures 4B, 4C, 4E, 4G, and 4H). These residues all are located within or immediately adjacent to the cryo-EM-determined footprint of CHK-265 (see structural analysis in Figure 5D) and thus comprise an epitope for broadly neutralizing MAbs.

When CHK-48, CHK-65, CHK-77, CHK-88, CHK-124, CHK-265, and 8I4 were tested for inhibition of RRV infection, they were poorly (CHK-65, CHK-77, CHK-88, and CHK-124), weakly (CHK-48 and 8I4), or only moderately (CHK-265) neutralizing (Figures 1C and 1H). To explore whether virus-specific amino acid differences in the epitope explained the reduced neutralization of RRV, we changed two residues in the E2 protein of the RRV cDNA clone to the corresponding CHIKV residues (184 [T→Q] and 185 [A→S]). The introduction of the two CHIKV amino acids into RRV resulted in improved binding and neutralization of RRV by CHK-48, CHK-65, CHK-77, CHK-88, CHK-124, CHK-187, and CHK-265 (Figures S4 and 4K–4Q). Engineering of two other CHIKV residues into RRV (192 [A→V] and 193 [G→N]) also improved binding (Figure S4) and neutralization (Figure 4R) of MAb CHK-98, which mapped to residues 189, 191, 192, and 193 in the B domain (Figure 3A).

Binding of B Domain MAbs Is Coincident with Structural Rearrangement of CHIKV E2

We determined the structure of CHIKV virions in complex with Fab fragments of CHK-265 by cryo-electron microscopy (cryo-EM) at ~16 Å resolution (Figure 5A). Three Fab molecules were bound to each of the q3 and i3 trimeric spikes within the 60 icosahedral asymmetric units. Unexpectedly, the virus density remaining after subtraction of the fitted CHK-265 Fab density could not be interpreted by fitting of the crystal structure of the E1-E2 heterodimer (Voss et al., 2010) (Figures S5A and S5B). Visual inspection suggested that the A and B domains in the

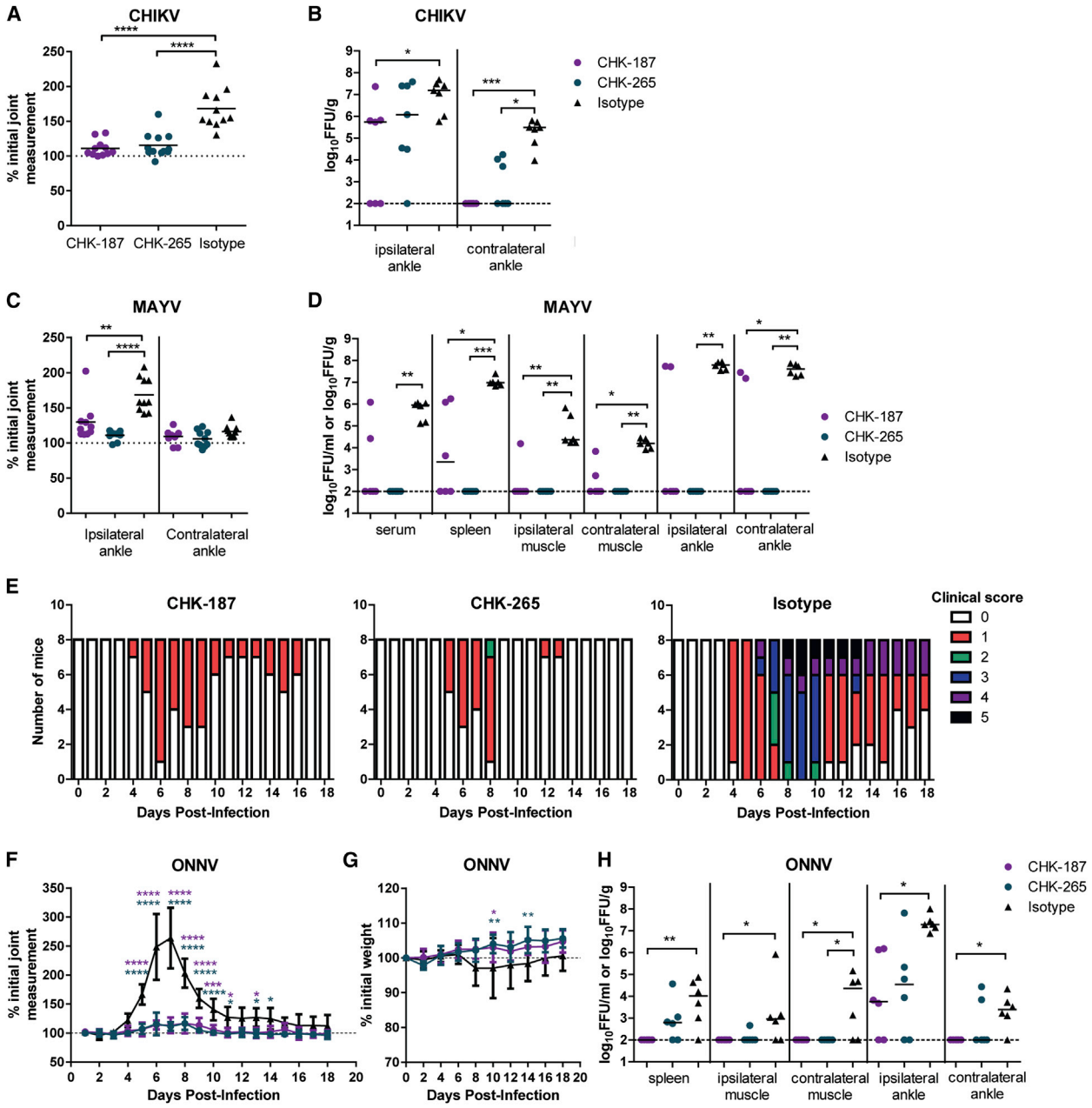

Figure 2. CHK-187 or CHK-265 Protect against Alphavirus Disease and Dissemination In Vivo

(A–D) Four-week-old WT mice were pretreated with 100 μg of CHK-187, CHK-265, or WNV E60 (isotype control) MAb 1 day prior to inoculation with 10^3 FFU of (A, B) CHIKV or (C, D) MAYV in the footpad. (A and C) Footpad swelling (width × height) in the ipsilateral and/or contralateral joint was measured prior to and 3 days following inoculation (n = 10 to 12). (B and D) Viral load was determined in indicated tissues 3 days following inoculation (n = 6–7).

(E–H) Six- to seven-week-old *Ifnar*$^{-/-}$ mice were administered MAbs as described above 1 day prior to inoculation with 10 FFU of ONNV in the footpad. (E) Mice (n = 8) were monitored for 18 days, and disease was scored as described in the Supplemental Experimental Procedures section. (F) Footpad swelling in the ipsilateral foot was followed during the course of infection (n = 8). (G) Weight was monitored each day and normalized to starting weight (n = 8). (H) The indicated tissues were collected 5 days after infection, and viral load was determined (n = 6).

For clinical measurements (panels A, C, F, and G), the mean and SD are shown, with the dashed line indicating the baseline prior to infection. For (A) and (C), statistical significance was determined by a one-way ANOVA with a Bonferroni post hoc test. For (F) and (G), statistical significance was determined by a two-way ANOVA with a Bonferroni post hoc test adjusting for repeated measures. For viral titers (B, D, and H), the median value is shown with the limit of sensitivity of the assay displayed as a dashed line. Statistical significance was determined by a Kruskal-Wallis with a Dunn's post hoc test. Each graph represents data obtained from at least two independent experiments (*$p < 0.05$, **$p < 0.01$, ***$p < 0.001$, ****$p < 0.0001$).

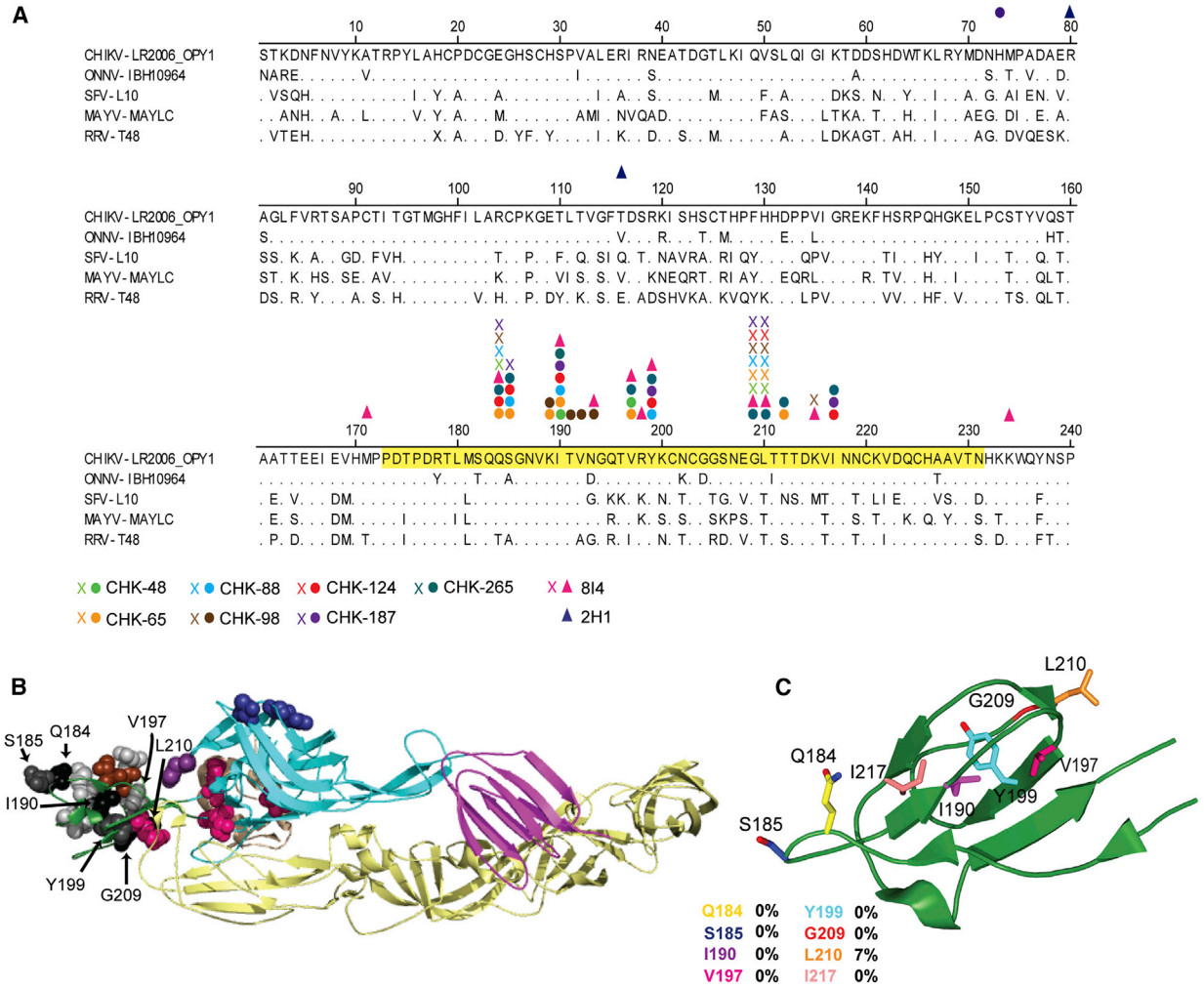

Figure 3. Broadly Neutralizing MAbs Map to Domain B of the E2 Protein

(A) CHIKV, ONNV, SFV, MAYV, and RRV were aligned using MegaAlign (DNA Star) with strain names following the virus. The B domain of CHIKV is highlighted in yellow. Residues mapped by alanine-scanning mutagenesis (see Figure S3) are in solid colored circles (mouse MAbs) or triangles (human MAbs). Additional residues identified as critical for MAb binding to the recombinant CHIKV E2 protein (Figure 4) are shown as an "X" in the MAb color.

(B) Mapped residues are shown as spheres on the CHIKV p62-E1 structure using PyMOL (PDB 3N42). Residues identified for a single MAb are indicated with a colored sphere corresponding to the MAb color in (A). Residues important for binding of multiple MAbs are colored in increasing shades of gray (light gray, 2–3 MAbs; medium gray, 4 MAbs; dark gray, 5 MAbs; and black, 7–8 MAbs). Residues identified for ≥4 MAbs are indicated on the E2 structure by an arrow. E1 is shown in yellow and E3 in tan. E2-A is in cyan, E2-B in dark green, and E2-C in purple.

(C) Blow-up of E2 B domain with key residues (≥3 MAbs with loss of binding) shown as sticks using Pymol (PDB: 3N42). The percent variation of amino acids in CHIKV strains is indicated to the right of the residue and was determined by aligning 415 different CHIKV E2 protein sequences.

See also Figure S3.

heterodimer had undergone substantial conformational change. To define this change, the A and B domains were removed from the crystal structure before fitting the remainder of the modified E1-E2 dimer, and then the A and B domains were fitted manually into the density using EMfit to maximize the average densities for each domain (Rossmann et al., 2001) (Table S3). This process showed that the position and orientation of the B domain had moved further over the fusion loop in domain II of E1 protein. In addition, the A domain had undergone a large repositioning (a translation of 21 Å and rotation of 71°) around the domain II of E1 (Figures 5B and S5C–S5E and Movies S1 and S2). In this new position, CHK-265 Fab binds the B domain on one spike and contacts the A domain on a neighboring spike, effectively cross-linking the spikes on the virion surface (Figure 5C and Movie S3); each q3 spike is linked to two neighboring q3 spikes and one i3 spike, and each i3 spike is linked to three neighboring q3 spikes. The C termini of the constant domains of Fab molecules that are bound to neighboring spikes make contacts with each other across quasi 2-fold axes in a manner consistent with the T4 quasi symmetry surface lattice. This result suggests that the intact CHK-265 IgG might be able to bind and cross-link many of the spikes together. The interface between CHK-265

and the virus consists of 19 residues in the B domain and 4 in the A domain (Figure 5D and Table S4). The cryo-EM-determined footprint of CHK-265 on the B domain (amino acids 180–220) is consistent with the identified loss- or gain-of-binding residues (e.g., Q184, S185, V192, N193, G209, and L210) from the mutagenesis-based strategies described above.

Broadly Neutralizing MAbs Inhibit Both Viral Entry and Egress

We evaluated the mechanism of inhibition for two broadly neutralizing MAbs, CHK-187 and CHK-265. Inhibition of viral attachment was assessed by pre-incubating CHK-187, CHK-265, or an isotype control MAb with CHIKV and then adding the mixture to cells at 4°C. CHK-187 and CHK-265 did not block viral attachment any more strongly than did the isotype control MAb (Figure 6A). Entry blockade was tested by pre-incubating CHIKV with CHK-187, CHK-265, or with the isotype control MAb and then allowing it to bind to cells at 37°C. One hour later, unbound virus and MAb were removed by extensive washing, and infectivity was assessed 18 hr later. Exposing CHIKV to CHK-187 and CHK-265 only at the time of entry resulted in neutralization that was comparable to when MAbs were maintained throughout infection, suggesting that entry blockade is a dominant mode of inhibition (Figure 6B). To determine whether MAb valency affected entry blockade, studies were repeated with Fab fragments. The Fab fragments were somewhat less potent (5- to 10-fold) than their IgG counterparts (Figure 6B). Saturating amounts of either CHK-187 or CHK-265 Fab fragments could not inhibit infection completely and resulted in a substantial neutralization-resistant fraction. This result suggests that, while monovalent binding of B domain MAbs can inhibit the entry step of infection, bivalent binding is required for complete neutralization.

Since CHK-187 and CHK-265 blocked at a post-attachment entry step, we tested whether they inhibited fusogenic activity using a liposomal fusion assay (Smit et al., 1999). Pyrene-labeled CHIKV was incubated with MAbs and mixed with liposomes, and a low-pH (5.1) buffer was added to trigger fusion. In contrast to results with potently neutralizing type-specific MAbs that bind preferentially to the A domain and completely block fusion (Pal et al., 2013), the cross-neutralizing B domain MAbs showed variable inhibition: fusion was blocked weakly (~20%) by CHK-187, moderately (~60%) by CHK-265, and more strongly (~80%) by CHK-88, although none inhibited completely (Figure 6C).

We next evaluated whether B domain MAbs also could block viral egress, presumably by inhibiting assembly or budding from the plasma membrane. Cells were inoculated with CHIKV and then washed extensively to remove free virus. Subsequently, CHK-187, CHK-265, or isotype control MAb was added, and viral RNA was analyzed from supernatants harvested at 1 or 6 hr; 6 hr corresponds to the initial round of virion secretion. Addition of CHK-187 or CHK-265 reduced the amount of CHIKV RNA in the supernatant compared to cells treated with the isotype control MAb (Figure 6D). Fab fragments of CHK-187 or CHK-265 were less potent than intact IgG, suggesting that cross-linking of E2 proteins on the cell or virion surface might contribute to blockade of egress (Figure 6E). To confirm these results, we transfected CHIKV RNA directly into cells, then added CHK-187, CHK-265, or isotype control MAb, and monitored accumulation of RNase-A-resistant encapsidated CHIKV RNA in the cells and supernatant. CHK-187 and CHK-265 had equivalent levels of intracellular viral RNA but had reduced accumulation of viral RNA in the supernatant compared to the isotype control MAb at 24 hr (Figure 6F). Finally, we determined the relative contribution of entry and egress blockade to cross-neutralization of MAYV. CHK-187 or CHK-265 inhibited MAYV infection at the entry (Figure 6G) and egress (Figure 6H) steps, although the effects on egress were less than that observed with CHIKV. Taken together, these results indicate that, while broadly neutralizing MAbs can inhibit multiple steps (including fusion and egress) in the alphavirus lifecycle, they preferentially cross-neutralize infection by blocking entry at a post-attachment pre-fusion step.

DISCUSSION

This study describes a panel of broadly neutralizing MAbs against multiple and distantly related arthritogenic alphaviruses. We identified ten mouse and human cross-neutralizing MAbs and showed that two of these MAbs protected in vivo against infection with homologous and heterologous alphaviruses. A conserved epitope in the B domain of the E2 protein contributed to the recognition of these broadly neutralizing MAbs. Structural analysis of CHIKV complexed with CHK-265 showed a large conformational change in the A domain of E2. Mechanistically, the B domain MAbs blocked CHIKV infection at both viral entry and egress steps, although the cross-neutralizing activity was due primarily to inhibition of entry. Collectively, these results describe a class of broadly neutralizing MAbs with substantive inhibitory activity against different members of the alphavirus genus.

We detected a larger number of broadly neutralizing mouse compared to human MAbs. While this could reflect a sampling bias of a small number of mice and a single human (Smith et al., 2015), it could suggest that the epitope repertoire is different between the species, as has been observed with antibodies against other viruses. In contrast to individuals who develop broadly neutralizing antibodies to HIV through constant exposure to the escaping viral envelope protein and extensive somatic hypermutation over time (Doria-Rose et al., 2014), sequencing of 8I4, the broadly neutralizing anti-alphavirus human MAb, revealed no evidence of such selection. Thus, selection for clones with specific and extensive somatic mutations, as required for HIV envelope protein antigens (Dosenovic et al., 2015), may not be required to elicit broadly neutralizing antibodies against alphaviruses.

Although CHK-187 and CHK-265 neutralized infection of CHIKV and MAYV equivalently in cell culture, greater protection in mice was observed against MAYV compared to CHIKV. The phenomenon in which an antibody raised against one virus protects to greater levels against a related virus was observed previously with flaviviruses. MAbs recognizing the conserved fusion loop of WNV E protein provided greater protection against DENV than WNV (Oliphant et al., 2006; Williams et al., 2013). In contrast to CHK-187 and CHK-265, the flavivirus-specific fusion loop-specific MAbs showed greater neutralizing activity in cell culture against DENV than WNV. The differences in protection in vivo

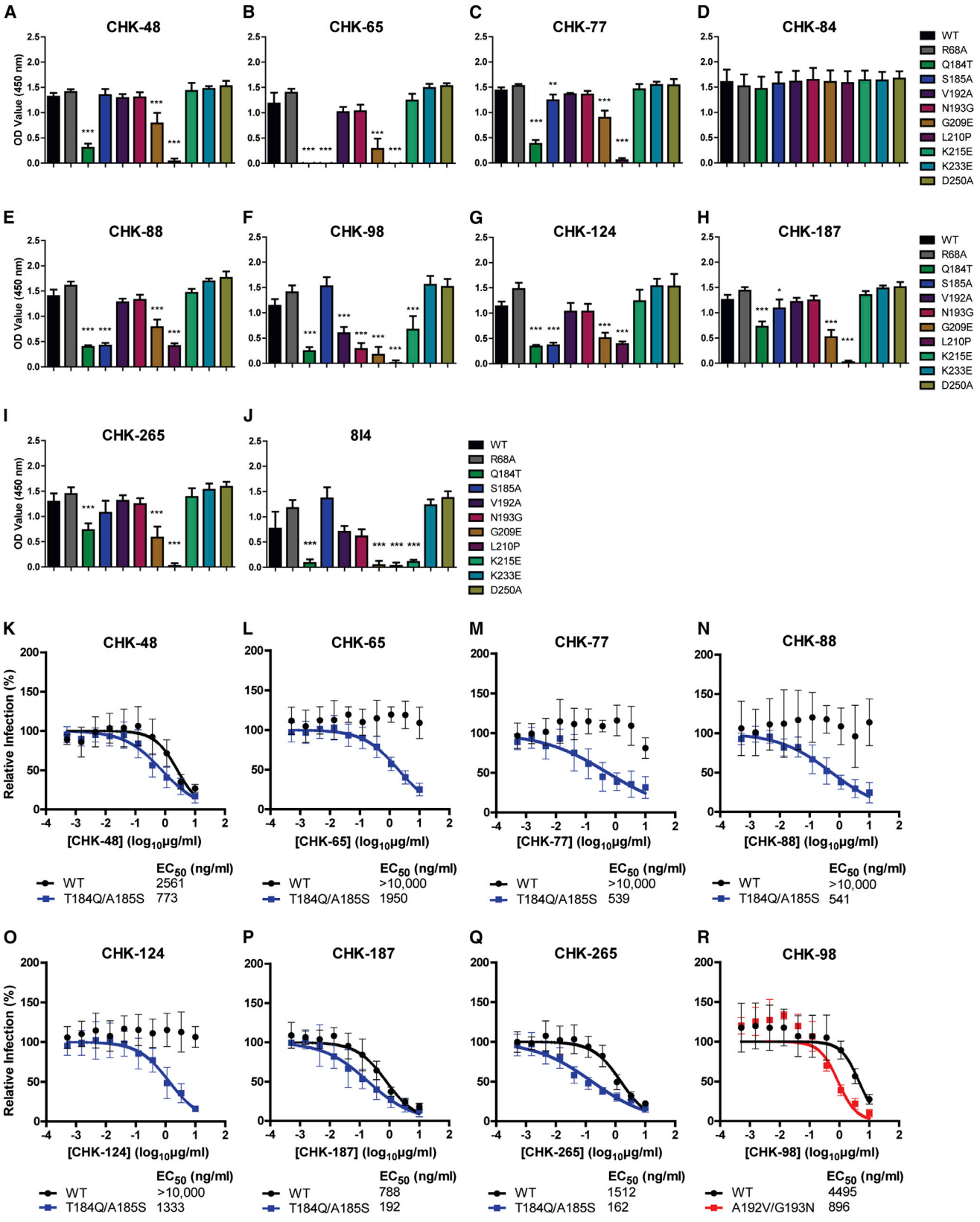

(legend on next page)

between CHIKV and MAYV with the same MAbs having equal neutralizing activity could reflect differences in tropism, pathogenesis, or propensity for accumulation of escape mutations with sustained virulence. Alternatively, the impact of effector functions (e.g., complement or antibody-dependent cellular cytotoxicity) on control of the different viruses could vary between models; these factors could be relevant especially for MAbs that block egress and bind to E1 or E2 proteins on the surface of infected cells.

Of the arthritogenic alphaviruses tested in this study, RRV had the greatest divergence in B domain sequence from CHIKV and, accordingly, was neutralized least efficiently by anti-CHIKV MAbs. MAbs that localize to the B domain on E2 of RRV have been reported to have neutralizing activity (Davies et al., 2000; Vrati et al., 1988), although their capacity for cross-neutralization was not assessed. Based on loss-of-binding studies with variant CHIKV E2 proteins, several key residues (Q184, S185, V192, N193, G209, and L210), all close to or within the cryo-EM determined footprint of CHK-265, contributed to the binding of broadly neutralizing anti-alphavirus MAbs. Four of these residues differed in RRV and, accordingly, substitution of the CHIKV amino acids at corresponding positions into RRV resulted in a gain-of-neutralization phenotype. Since RRV and CHIKV currently do not circulate in the same endemic regions, it seems unlikely that RRV evolved these changes to evade pre-existing immunity against CHIKV.

Our findings with B domain MAbs may be relevant in the context of vaccination, as cross-neutralization of different alphaviruses by polyclonal antibodies has been observed. Cross-protection by anti-RRV serum against CHIKV infection and anti-CHIKV serum against ONNV infection was reported in mice (Gardner et al., 2010; Partidos et al., 2012). However, serum or MAbs derived from ONNV-infected animals or humans weakly neutralized CHIKV (Blackburn et al., 1995; Porterfield, 1961). Future genetic analysis paired with reagents that deplete cross-neutralizing B domain antibodies in serum is needed to explain fully the basis for the directionality of inhibition of polyclonal serum of different alphaviruses.

Cryo-EM structures of several alphaviruses have shown that the B domain has a lower electron density, implying that its position varies by roughly 4 Å relative to the best average orientation of the icosahedral symmetry axes (Porta et al., 2014; Sun et al., 2013). Similarly, the B domain is disordered in the low-pH crystal structure of CHIKV trimeric spikes (Li et al., 2010) and has a high "temperature" factor in the crystal structure of the CHIKV E2-E1 heterodimer (Voss et al., 2010). This structural feature is important because the fusion loop on domain II of the E1 protein is hidden under the B domain to prevent adventitious fusion. Thus, the capacity for the B domain to move likely is required for the fusogenic activity of the CHIKV. In the cryo-EM map of CHIKV complexed with CHK-265, the B domain had an electron density height equal to the other glycoprotein domains in all four quasi-equivalent positions within the icosahedral asymmetric unit. This configuration likely occurs because the Fab fragment bridges the normally flexible B domain to a second contact site in the more stable A domain. With the B domains tethered, it is more difficult for the fusion loops in E1 to be exposed, which might explain the observed partial inhibition of viral fusion. Another unusual feature of the cryo-EM map is that domain I of E1 has lower density than the other domains, implying a greater flexibility. This domain connects domain II to domain III of E1 that forms the base of the spike. A flexible domain I might result in a floppy trimeric spike, which could impair entry functions of the virus.

In a previous study with Fab fragments of four different MAbs bound to CHIKV-like particles, binding did not cause major conformational changes to the structure of the virus (Sun et al., 2013). These antibodies bound primarily to the A domain of E2. In contrast, CHK-265 Fab binding is centered in the B domain and is coincident with large conformational changes. The cryo-EM analysis of the CHK-265-virion complex showed that although the orientation of the A domain is changed radically, the putative receptor binding site (Sun et al., 2013) remains accessible. This finding is consistent with the observation that CHIKV can attach efficiently to cells in the presence of CHK-265. Binding of CHK-265 induced a conformational shift of the four quasi T-4 related A domains to sites between neighboring spikes, consistent with the T = 4 quasi-symmetry. Although mutagenesis studies did not identify residues in the A domain that resulted in loss of binding of CHK-265, amino acid H73 in domain A of E2 contributed to the binding of the broadly neutralizing MAb CHK-187. This residue is present in the cryo-EM-determined binding footprint of CHK-265.

Vaccine- and antibody-based therapy efforts against HIV, IAV, and DENV have focused on the induction or generation of neutralizing antibodies that target most strains of a virus within a given genus. These broadly neutralizing antibodies function by binding to conserved glycans, receptor-binding domains, stem regions, or dimer and trimer contacts of the envelope glycoproteins (Corti and Lanzavecchia, 2013). Our description of a class of MAbs that induces marked structural changes in the virion, inhibits infection at multiple steps in the viral lifecycle, and protects in vivo against disease pathogenesis by multiple alphaviruses suggests that targeting of the B domain on E2 could serve as a strategy for the development of vaccines with utility against CHIKV and several related viruses of global concern.

Figure 4. Mutation of Domain B Residues Eliminates Binding to CHIKV E2 and Enhances Neutralization of RRV

(A–J) Mutations were introduced into the CHIKV E2 ectodomain, and binding was determined by ELISA. Significant reduction compared to the WT E2 protein was determined by a one-way ANOVA with Dunnett's multiple comparison tests (*$p < 0.05$, **$p < 0.01$, ***$p < 0.001$).

(K–R) Serial dilutions of MAbs were incubated with 10^2 FFU of RRV-WT, RRV-T184Q/A185S, or RRV-A192V/G193N for 1 hr at 37°C followed by addition of MAb-virus mixture to Vero cells for 18 hr. Cells were fixed, and virally infected foci were stained. Wells containing MAb were compared to wells containing no MAb to determine the relative infection. EC_{50} values are shown as ng/ml. Each graph shows the mean and SD from two to three independent experiments performed in duplicate.

See also Figure S4.

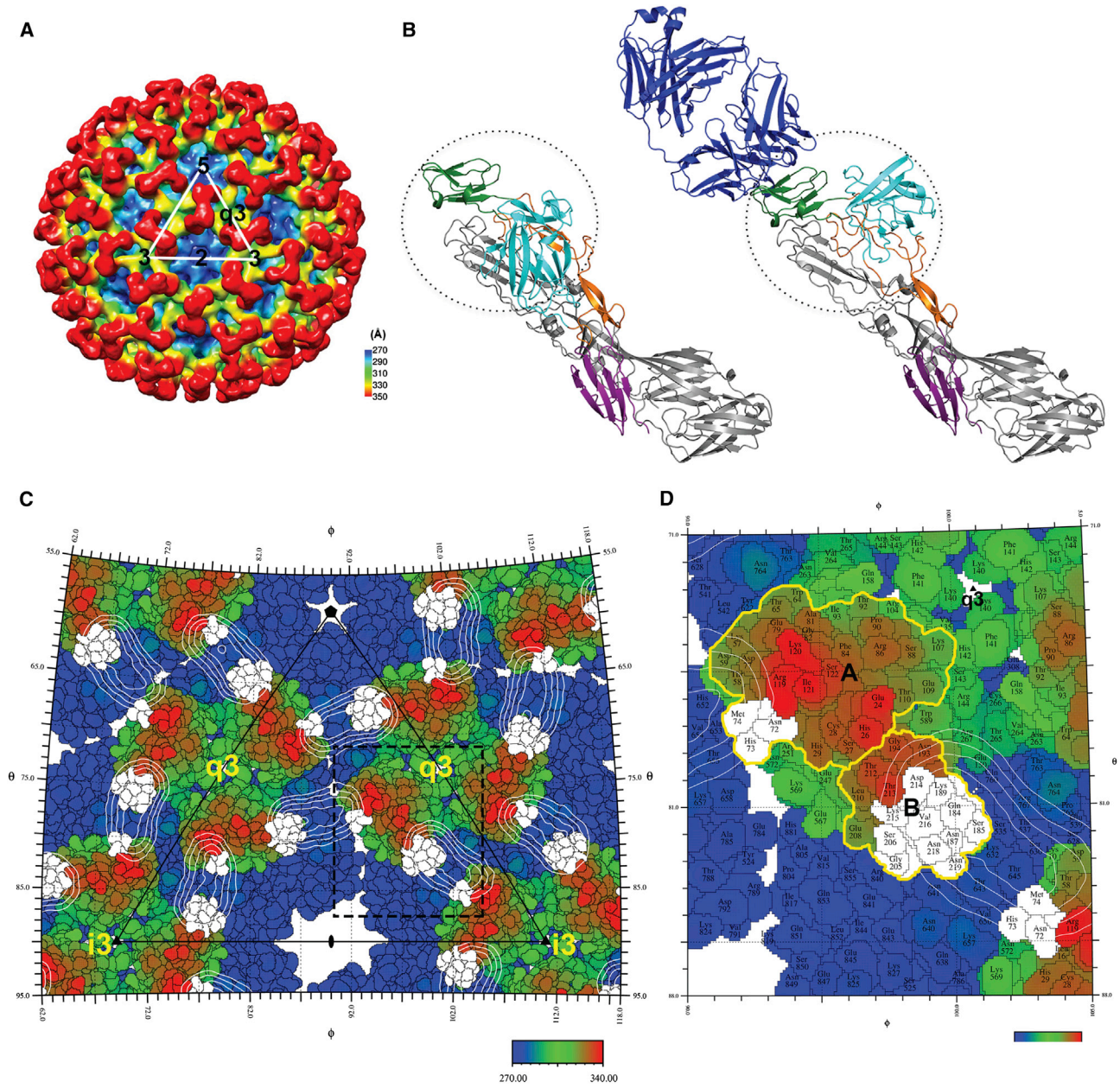

Figure 5. CHK-265 Binding to CHIKV Results in Repositioning of the E2 A Domain

(A) Cryo-EM reconstruction of CHIKV 181/25 in complex with CHK-265 Fab fragments. The triangle represents one icosahedral asymmetric unit. The colors indicate the radial distance in Å from the center of the virus, as shown on the scale bar.

(B) (Left) Structure of the E1-E2 heterodimer (PDB: 3N42). (Right) Structure of the E1-E2 heterodimer with the bound Fab molecule, as observed in the cryo-EM complex of the virus with CHK-265. The CHK-265 Fab molecule is colored blue, and the CHIKV E1-E2 heterodimer (PDB: 3N42) is colored with E1 in gray, E2-A in cyan, E2-B in green, E2-C in purple, and the E2-β-ribbon in orange. The left and right ribbon structures are oriented to place the lower parts of these figures (E1 and domain E2-C) into the same orientation. The E2 A and E2 B domains are circled, showing the difference in their conformations.

(C) Roadmap showing footprint of CHK-265 Fab projected onto the surface of CHIKV. The projections are colored according to the radial distance of the surface from the center of the virus, as shown in the scale bar. The white contours are the radial projections of the bound Fab molecules onto the surface of the virus. The black triangle denotes the boundary of an icosahedral asymmetric unit. The 5-fold, 3-fold, and 2-fold icosahedral axes are indicated by a small black pentagon, triangle, and oval symbol, respectively. The residues in the Fab footprints are shown in white. Each Fab footprint bridges separate trimers with the variable portion of the Fab binding to the E2-B domain on one spike and the E2-A domain on a neighboring spike.

(D) Enlargement of a part of the q3 spike shown on the right in (C). The A and B domains of E2 are outlined in yellow. Individual surface amino acids are labeled and outlined in black. To differentiate residues in E1 from those in E2, a value of 500 arbitrarily was added to the E1 residue numbers. The roadmaps were created by the program RIVEM (Xiao and Rossmann, 2007).

See also Figure S5, Table S3 and S4, and Movies S1, S2, and S3.

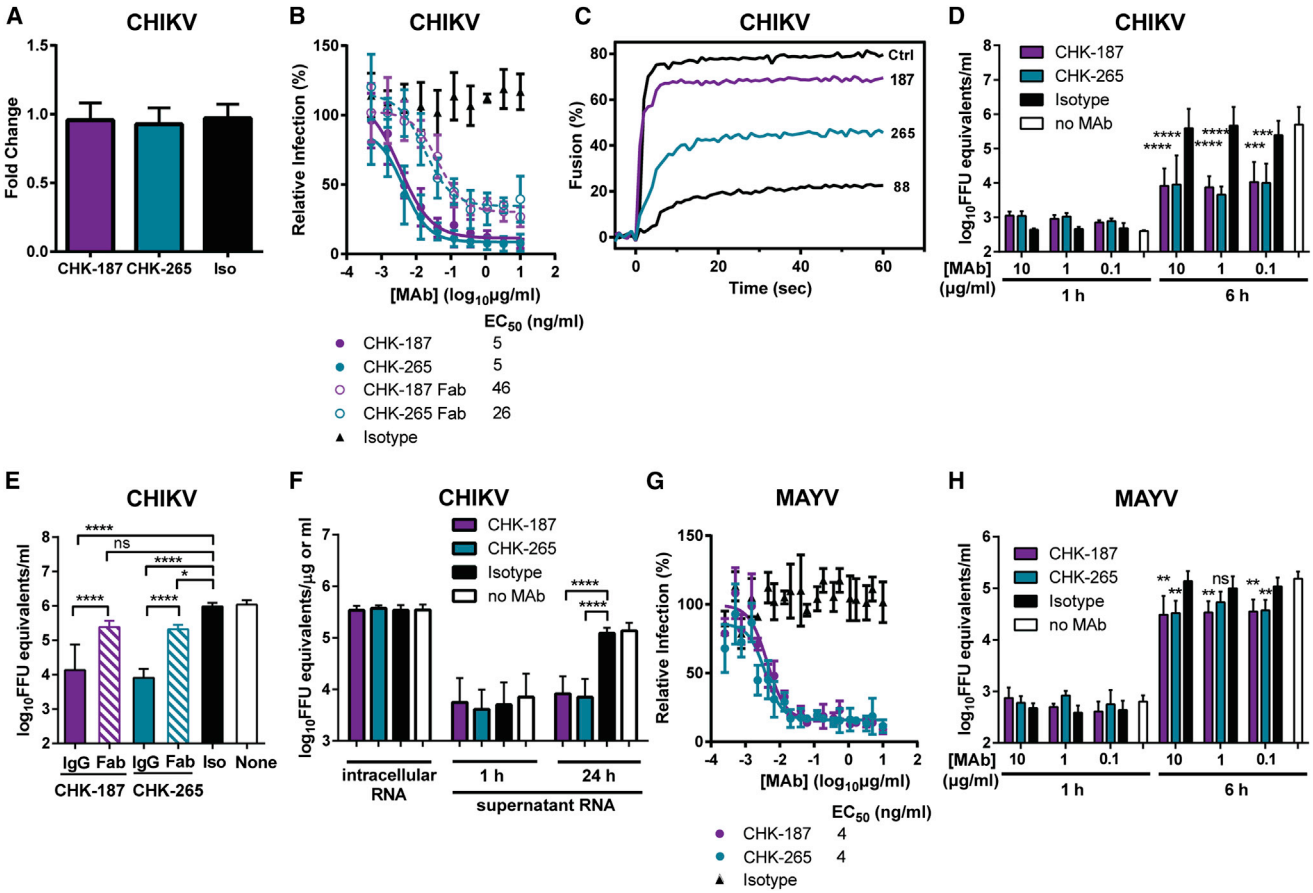

Figure 6. Broadly Neutralizing Anti-CHIKV MAbs Block Steps in Viral Entry and Egress

(A–F) Mechanism of action studies with CHIKV. (A) Attachment blockade. CHIKV was incubated with CHK-187, CHK-265, or isotype control MAb (Iso; WNV E60) for 1 hr, added to chilled Vero cells for 1 hr at 4°C, and washed extensively, and bound CHIKV viral RNA was measured. RNA levels are normalized to a no MAb treatment control. (B) Entry blockade. 10^2 FFU of CHIKV were incubated with indicated MAbs or Fabs at 37°C for 1 hr, added to Vero cells for 1 hr at 37°C, washed extensively, overlaid with methylcellulose, and fixed 18 hr later. Wells containing MAb were compared to wells containing no MAb to determine the relative infection. (C) Fusion blockade. Pyrene-labeled CHIKV was incubated with 1.5 μg/ml of the indicated MAbs and mixed with liposomes at 37°C, and fusion was triggered with a low-pH (5.1) buffer. The percent fusion was measured over time compared to a no MAb control. (D–F) Egress blockade. Vero cells were inoculated with (D, E) CHIKV for 2 hr at 37°C and rinsed extensively, and medium containing (D, E) IgG or (E) Fab fragments (10 μg/ml) and 25 mM NH_4Cl was added back. Supernatant was collected 1 or 6 hr later, the latter of which corresponds to the first round of virion production, and was analyzed for CHIKV viral RNA. (F) BHK21 cells were transfected with CHIKV RNA and rinsed extensively, and medium containing 10 μg/ml IgG and 25 mM NH_4Cl was added. Cells and supernatants were collected 1 or 24 hr later, treated with RNase A at 37°C to degrade unencapsidated RNA, and analyzed for CHIKV viral RNA. See Figure S6 for additional controls.

(G and H) Mechanism of action studies with MAYV. (G). Entry blockade. Studies were performed as described above in (B) using 10^2 FFU of MAYV. (H) Egress blockade. Studies were performed as described above in (D) using MAYV at an MOI of 1 and analyzed for MAYV viral RNA.

Graphs in this figure show the mean and SD of two or three independent experiments performed in triplicate or duplicate. EC_{50} values for entry blockade are shown as ng/ml and were determined by non-linear regression. Statistical significance for the egress blockade assay was determined using a one-way ANOVA with a Bonferroni post hoc test at each MAb concentration and time point (*$p < 0.05$, **$p < 0.01$, ***$p < 0.001$, ****$p < 0.0001$).

EXPERIMENTAL PROCEDURES

Antibodies, Cell Culture, and Viruses

Mouse and human MAbs against CHIKV were reported previously (Pal et al., 2013; Smith et al., 2015) and were purified by Protein A Sepharose and S200 size-exclusion chromatography. Purified CHK-265 and CHK-187 were digested with papain (Pierce) to generate Fab fragments and were collected in the flow-through after passage over a Protein A Sepharose column. Vero, BHK21, and C6/36 cells were cultured as described (Pal et al., 2013). CHIKV (La Reunion OPY1 p142) and RRV (T48) were the gifts of S. Higgs (Kansas State University) and R. Kuhn (Purdue University), respectively, and were produced from infectious cDNA clones (Morrison et al., 2006; Tsetsarkin et al., 2006). MAYV (BeH407), ONNV (MP30), SFV (Kumba), BEBV (MM 2354), MIDV (30037), GETV (AMM-2021), UNAV (CoAr2380), and BFV (K10521) were provided by the World Reference Center for Arboviruses and propagated in Vero cells.

Focus Reduction Neutralization Assay

Focus reduction neutralization tests (FRNT) were performed as described (Pal et al., 2013). Additional details are reported in the Supplemental Experimental Procedures.

Mouse Studies

Experiments were carried out in accordance with the recommendations in the Guide for the Care and Use of Laboratory Animals of the National Institutes of

Health after approval by the Institutional Animal Care and Use Committee at the Washington University School of Medicine. MAbs CHK-187 or CHK-265 or isotype control MAb WNV E60 (100 μg in PBS, 6 mg/kg) were administered to 4-week-old WT C57BL/6 mice or 6- to 7-week old *Ifnar*$^{-/-}$ mice by intraperitoneal injection 1 day prior to infection. WT mice were infected subcutaneously in the footpad with CHIKV or MAYV. *Ifnar*$^{-/-}$ mice were inoculated in the footpad with ONNV. Animals were scored daily using a modified clinical disease scale created for RRV (Morrison et al., 2006). Additional information is in the Supplemental Experimental Procedures.

Mutagenesis of CHIKV E2 and ELISA

Amino acid substitutions were introduced into the CHIKV E2 ectodomain (residues S1-E361) using Quikchange II mutagenesis (Aligent) and the primers listed in Table S1. Mutations were confirmed by direct sequencing of plasmid DNA. MAb binding to CHIKV WT or mutant E2 proteins was assessed by ELISA. Detailed protocols are described in the Supplemental Experimental Procedures.

Mutagenesis of RRV Infectious Clone

A double mutation at positions 192(A→V) and 193(G→N) of the E2 gene was introduced into the pRR64 cDNA clone of RRV by Quikchange II mutagenesis (Aligent). Double mutations at positions 184(T→Q) and 185(A→S) of the E2 gene were engineered using Phusion high-fidelity DNA polymerase (New England BioLabs). The mutagenesis primers are listed in Table S1. Mutations were confirmed by sequencing with separate primers (Table S2). WT and mutant RRV were produced after plasmid linearization, in vitro transcription, and electroporation into BHK21 cells. Additional details of RRV mutagenesis are provided in the Supplemental Experimental Procedures.

Cryo-EM Reconstruction of CHK-265 in Complex with CHIKV

Purified CHK-265 Fab molecules (5 mg/ml) were mixed with purified and concentrated CHIKV (181/25) in 2:1 (Fab:E2) molar ratio and incubated on ice for 30 min. Samples were flash frozen on holey carbon grids (Ted Pella) in liquid ethane using Cryo-plunge 3 (CP3) in a biosafety cabinet. CCD images of the CHIKV-Fab complex were recorded under low-dose conditions (~22 e/Å^2) using a FEI Titan Krios electron microscope operated at 300 kV and 47,000× magnification. All cryo-EM images were collected at about 1.5–3 μm below the focus level. A total of 5,828 particles was selected manually with the e2boxer program in the EMAN2 suite (Kimoto et al., 2003; Tang et al., 2007). Contrast levels of micrographs were corrected using the ctfit program in EMAN (Ludtke et al., 1999; Tang et al., 2007). Additional information about the purification of CHIKV and CHK-265 Fabs and the cryo-EM model generation is described in the Supplemental Experimental Procedures.

Mechanistic Analyses of MAb Inhibition

(a) For virus attachment inhibition assays, MAbs were incubated with CHIKV at 37°C, chilled, and added to pre-cooled Vero cells. Cells were extensively rinsed, and bound RNA was extracted from the cells and measured by qRT-PCR. (b) For entry inhibition assays, MAbs or Fabs were incubated with virus at 37°C, added to Vero cells, and after extensive rinsing, processed as described for the FRNT assay. (c) Liposomal fusion inhibition assays were performed as described (Pal et al., 2013). (d) For egress inhibition assays, Vero and BHK21 cells were infected with virus or transfected with viral RNA, respectively. Cells were rinsed extensively, and MAbs or Fabs were added in medium containing NH_4Cl. Viral RNA was quantified from supernatant or cells. Detailed protocols are described in the Supplemental Experimental Procedures.

ACCESSION NUMBERS

The cryo-EM density map of CHIKV in complex with CHK-265 Fab fragments was deposited with the EM Data Bank under accession number EMD: EMD-3144. The coordinates of the fitted structural models of CHK-265 Fab and E1-E2 were deposited with the Protein Data Bank under accession number PDB: 5ANY.

SUPPLEMENTAL INFORMATION

Supplemental Information includes Supplemental Experimental Procedures, six figures, four tables, and three movies and can be found with this article online at http://dx.doi.org/10.1016/j.cell.2015.10.050.

AUTHOR CONTRIBUTIONS

J.M.F., F.L., H.L., M.K.S.v.D.-R., R.H.F., and K.M.K. performed the experiments. J.M.F., F.L., H.L., M.K.S.v.D-.R, K.M.K., J.M.S., B.J.D., M.A.E., J.E.C., D.H.F., M.G.R., and M.S.D. designed the experiments and analyzed the data. M.A.E., J.E.C., J.J., and G.S. contributed key reagents and methodology. J.M.F., F.L., J.E.C., M.G.R., and M.S.D. wrote the first draft of the manuscript, and all authors provided editorial suggestions and criticisms.

ACKNOWLEDGMENTS

This work was supported by National Institutes of Health (NIH) grants R01 AI095366 (M.G.R.), R01 AI089591 (M.S.D.), HHSN272200900055C (B.J.D.), T32 AI007172 (J.M.F.), and R01 AI114816 (J.E.C. and M.S.D.); the Dutch Organization for Scientific Research (NWO–Earth and Life Sciences) (J.M.S.); the University Medical Center Groningen (M.K.S.v.D.-.R.); and a NRSA-Infectious Diseases training grant (J.M.F.). The authors thank S. Johnson (MacroGenics) and G. Sapparapu (Vanderbilt University) for providing purified MAbs, R. Tesh for providing many of the alphaviruses used in this study, P. Pal for the initial cross-reactivity studies, and K. O'Brien and N. DiStasio for technical assistance with mutant E2 protein production and epitope mapping. J.E.C. and M.S.D. have been consultants for Sanofi-Pasteur, which has an agreement with Vanderbilt University to evaluate antibody-based therapeutics against CHIKV. R.H.F, K.M.K, and B.J.D. are employees of Integral Molecular, and B.J.D. is a shareholder of Integral Molecular.

Received: July 30, 2015
Revised: September 18, 2015
Accepted: October 19, 2015
Published: November 5, 2015

REFERENCES

Blackburn, N.K., Besselaar, T.G., and Gibson, G. (1995). Antigenic relationship between chikungunya virus strains and o'nyong nyong virus using monoclonal antibodies. Res. Virol. *146*, 69–73.

Cheng, R.H., Kuhn, R.J., Olson, N.H., Rossmann, M.G., Choi, H.K., Smith, T.J., and Baker, T.S. (1995). Nucleocapsid and glycoprotein organization in an enveloped virus. Cell *80*, 621–630.

Corti, D., and Lanzavecchia, A. (2013). Broadly neutralizing antiviral antibodies. Annu. Rev. Immunol. *31*, 705–742.

Couderc, T., Khandoudi, N., Grandadam, M., Visse, C., Gangneux, N., Bagot, S., Prost, J.F., and Lecuit, M. (2009). Prophylaxis and therapy for Chikungunya virus infection. J. Infect. Dis. *200*, 516–523.

Davidson, E., and Doranz, B.J. (2014). A high-throughput shotgun mutagenesis approach to mapping B-cell antibody epitopes. Immunology *143*, 13–20.

Davies, J.M., Cai, Y.P., Weir, R.C., and Rowley, M.J. (2000). Characterization of epitopes for virus-neutralizing monoclonal antibodies to Ross River virus E2 using phage-displayed random peptide libraries. Virology *275*, 67–76.

Doria-Rose, N.A., Schramm, C.A., Gorman, J., Moore, P.L., Bhiman, J.N., DeKosky, B.J., Ernandes, M.J., Georgiev, I.S., Kim, H.J., Pancera, M., et al.; NISC Comparative Sequencing Program (2014). Developmental pathway for potent V1V2-directed HIV-neutralizing antibodies. Nature *509*, 55–62.

Dosenovic, P., von Boehmer, L., Escolano, A., Jardine, J., Freund, N.T., Gitlin, A.D., McGuire, A.T., Kulp, D.W., Oliveira, T., Scharf, L., et al. (2015). Immunization for HIV-1 Broadly Neutralizing Antibodies in Human Ig Knockin Mice. Cell *161*, 1505–1515.

Fong, R.H., Banik, S.S., Mattia, K., Barnes, T., Tucker, D., Liss, N., Lu, K., Selvarajah, S., Srinivasan, S., Mabila, M., et al. (2014). Exposure of epitope

residues on the outer face of the chikungunya virus envelope trimer determines antibody neutralizing efficacy. J. Virol. *88*, 14364–14379.

Fric, J., Bertin-Maghit, S., Wang, C.I., Nardin, A., and Warter, L. (2013). Use of human monoclonal antibodies to treat Chikungunya virus infection. J. Infect. Dis. *207*, 319–322.

Gardner, J., Anraku, I., Le, T.T., Larcher, T., Major, L., Roques, P., Schroder, W.A., Higgs, S., and Suhrbier, A. (2010). Chikungunya virus arthritis in adult wild-type mice. J. Virol. *84*, 8021–8032.

Goh, L.Y., Hobson-Peters, J., Prow, N.A., Gardner, J., Bielefeldt-Ohmann, H., Pyke, A.T., Suhrbier, A., and Hall, R.A. (2013). Neutralizing monoclonal antibodies to the E2 protein of chikungunya virus protects against disease in a mouse model. Clin. Immunol. *149*, 487–497.

Kam, Y.W., Lum, F.M., Teo, T.H., Lee, W.W., Simarmata, D., Harjanto, S., Chua, C.L., Chan, Y.F., Wee, J.K., Chow, A., et al. (2012). Early neutralizing IgG response to Chikungunya virus in infected patients targets a dominant linear epitope on the E2 glycoprotein. EMBO Mol. Med. *4*, 330–343.

Kendrick, K., Stanek, D., and Blackmore, C.; Centers for Disease Control and Prevention (CDC) (2014). Notes from the field: Transmission of chikungunya virus in the continental United States–Florida, 2014. MMWR Morb. Mortal. Wkly. Rep. *63*, 1137.

Kimoto, K., Ishizuka, K., Tanaka, N., and Matsui, Y. (2003). Practical procedure for coma-free alignment using caustic figure. Ultramicroscopy *96*, 219–227.

Lescar, J., Roussel, A., Wien, M.W., Navaza, J., Fuller, S.D., Wengler, G., Wengler, G., and Rey, F.A. (2001). The Fusion glycoprotein shell of Semliki Forest virus: an icosahedral assembly primed for fusogenic activation at endosomal pH. Cell *105*, 137–148.

Li, L., Jose, J., Xiang, Y., Kuhn, R.J., and Rossmann, M.G. (2010). Structural changes of envelope proteins during alphavirus fusion. Nature *468*, 705–708.

Ludtke, S.J., Baldwin, P.R., and Chiu, W. (1999). EMAN: semiautomated software for high-resolution single-particle reconstructions. J. Struct. Biol. *128*, 82–97.

Lum, F.M., Teo, T.H., Lee, W.W., Kam, Y.W., Rénia, L., and Ng, L.F. (2013). An essential role of antibodies in the control of Chikungunya virus infection. J. Immunol. *190*, 6295–6302.

Morrison, T.E., Whitmore, A.C., Shabman, R.S., Lidbury, B.A., Mahalingam, S., and Heise, M.T. (2006). Characterization of Ross River virus tropism and virus-induced inflammation in a mouse model of viral arthritis and myositis. J. Virol. *80*, 737–749.

Morrison, T.E., Oko, L., Montgomery, S.A., Whitmore, A.C., Lotstein, A.R., Gunn, B.M., Elmore, S.A., and Heise, M.T. (2011). A mouse model of chikungunya virus-induced musculoskeletal inflammatory disease: evidence of arthritis, tenosynovitis, myositis, and persistence. Am. J. Pathol. *178*, 32–40.

Oliphant, T., Nybakken, G.E., Engle, M., Xu, Q., Nelson, C.A., Sukupolvi-Petty, S., Marri, A., Lachmi, B.E., Olshevsky, U., Fremont, D.H., et al. (2006). Antibody recognition and neutralization determinants on domains I and II of West Nile Virus envelope protein. J. Virol. *80*, 12149–12159.

Pal, P., Dowd, K.A., Brien, J.D., Edeling, M.A., Gorlatov, S., Johnson, S., Lee, I., Akahata, W., Nabel, G.J., Richter, M.K., et al. (2013). Development of a highly protective combination monoclonal antibody therapy against Chikungunya virus. PLoS Pathog. *9*, e1003312.

Pal, P., Fox, J.M., Hawman, D.W., Huang, Y.J., Messaoudi, I., Kreklywich, C., Denton, M., Legasse, A.W., Smith, P.P., Johnson, S., et al. (2014). Chikungunya viruses that escape monoclonal antibody therapy are clinically attenuated, stable, and not purified in mosquitoes. J. Virol. *88*, 8213–8226.

Partidos, C.D., Paykel, J., Weger, J., Borland, E.M., Powers, A.M., Seymour, R., Weaver, S.C., Stinchcomb, D.T., and Osorio, J.E. (2012). Cross-protective immunity against o'nyong-nyong virus afforded by a novel recombinant chikungunya vaccine. Vaccine *30*, 4638–4643.

Porta, J., Jose, J., Roehrig, J.T., Blair, C.D., Kuhn, R.J., and Rossmann, M.G. (2014). Locking and blocking the viral landscape of an alphavirus with neutralizing antibodies. J. Virol. *88*, 9616–9623.

Porterfield, J.S. (1961). Cross-neutralization studies with group A arthropod-borne viruses. Bull. World Health Organ. *24*, 735–741.

Rossmann, M.G., Bernal, R., and Pletnev, S.V. (2001). Combining electron microscopic with x-ray crystallographic structures. J. Struct. Biol. *136*, 190–200.

Roussel, A., Lescar, J., Vaney, M.C., Wengler, G., Wengler, G., and Rey, F.A. (2006). Structure and interactions at the viral surface of the envelope protein E1 of Semliki Forest virus. Structure *14*, 75–86.

Schilte, C., Staikowsky, F., Couderc, T., Madec, Y., Carpentier, F., Kassab, S., Albert, M.L., Lecuit, M., and Michault, A. (2013). Chikungunya virus-associated long-term arthralgia: a 36-month prospective longitudinal study. PLoS Negl. Trop. Dis. *7*, e2137.

Seymour, R.L., Rossi, S.L., Bergren, N.A., Plante, K.S., and Weaver, S.C. (2013). The role of innate versus adaptive immune responses in a mouse model of O'nyong-nyong virus infection. Am. J. Trop. Med. Hyg. *88*, 1170–1179.

Smit, J.M., Bittman, R., and Wilschut, J. (1999). Low-pH-dependent fusion of Sindbis virus with receptor-free cholesterol- and sphingolipid-containing liposomes. J. Virol. *73*, 8476–8484.

Smith, T.J., Cheng, R.H., Olson, N.H., Peterson, P., Chase, E., Kuhn, R.J., and Baker, T.S. (1995). Putative receptor binding sites on alphaviruses as visualized by cryoelectron microscopy. Proc. Natl. Acad. Sci. USA *92*, 10648–10652.

Smith, S.A., Silva, L.A., Fox, J.M., Flyak, A.I., Kose, N., Sapparapu, G., Khomadiak, S., Ashbrook, A.W., Kahle, K.M., Fong, R.H., et al. (2015). Isolation and Characterization of Broad and Ultrapotent Human Monoclonal Antibodies with Therapeutic Activity against Chikungunya Virus. Cell Host Microbe *18*, 86–95.

Sun, S., Xiang, Y., Akahata, W., Holdaway, H., Pal, P., Zhang, X., Diamond, M.S., Nabel, G.J., and Rossmann, M.G. (2013). Structural analyses at pseudo atomic resolution of Chikungunya virus and antibodies show mechanisms of neutralization. eLife *2*, e00435.

Tang, G., Peng, L., Baldwin, P.R., Mann, D.S., Jiang, W., Rees, I., and Ludtke, S.J. (2007). EMAN2: an extensible image processing suite for electron microscopy. J. Struct. Biol. *157*, 38–46.

Tsetsarkin, K., Higgs, S., McGee, C.E., De Lamballerie, X., Charrel, R.N., and Vanlandingham, D.L. (2006). Infectious clones of Chikungunya virus (La Réunion isolate) for vector competence studies. Vector Borne Zoonotic Dis. *6*, 325–337.

Voss, J.E., Vaney, M.C., Duquerroy, S., Vonrhein, C., Girard-Blanc, C., Crublet, E., Thompson, A., Bricogne, G., and Rey, F.A. (2010). Glycoprotein organization of Chikungunya virus particles revealed by X-ray crystallography. Nature *468*, 709–712.

Vrati, S., Fernon, C.A., Dalgarno, L., and Weir, R.C. (1988). Location of a major antigenic site involved in Ross River virus neutralization. Virology *162*, 346–353.

Williams, K.L., Sukupolvi-Petty, S., Beltramello, M., Johnson, S., Sallusto, F., Lanzavecchia, A., Diamond, M.S., and Harris, E. (2013). Therapeutic efficacy of antibodies lacking Fcγ receptor binding against lethal dengue virus infection is due to neutralizing potency and blocking of enhancing antibodies [corrected]. PLoS Pathog. *9*, e1003157.

Wust, C.J., Crombie, R., and Brown, A. (1987). Passive protection across subgroups of alphaviruses by hyperimmune non-cross-neutralizing anti-Sindbis serum. Proc. Soc. Exp. Biol. Med. *184*, 56–63.

Xiao, C., and Rossmann, M.G. (2007). Interpretation of electron density with stereographic roadmap projections. J. Struct. Biol. *158*, 182–187.